Eighth Australasian Fluid Mechanics Conference, University of Newcastle, N.S.W., 28 November/2 December 1983.

AERODYNAMIC DAMPING OF A CIRCULAR CYLINDER IN TURBULENT FLOW AT HIGH REYNOLDS NUMBERS

J.C.K. CHEUNG AND W.H. MELBOURNE

DEPARTMENT OF MECHANICAL ENGINEERING

MONASH UNIVERSITY, CLAYTON, VIC. 3168 AUSTRALIA

SUMMARY Experimental technique to measure the aerodynamic damping for a circular cylinder in uniform flows of different turbulent intensities, different Reynolds numbers, different velocity ratios and for different amplitudes of the cylinder motion is described. Existing published results from experiments in subcritical smooth flow conditions and from compilation by other previous studies are compared with the present data. These new data can be used together with some other aerodynamic parameters in a mathematical model to predict the cross-wind response of a circular structure like a chimney stack free-standing in wind.

1 NOTATION

D	diameter
I_u	longitudinal turbulence intensity
K_a	$\left(= \frac{-m\left(\frac{\delta_a}{2\pi}\right)}{\rho D^2}\right)$ aerodynamic damping parameter
K_{a_o}	aerodynamic damping parameter for stationary cylinder
L_x	longitudinal integral length scale of turbulence
m	mass per unit length
Re	Reynolds number
U	mean wind speed
$U_{crit.}$	critical velocity when the vortex shedding frequency equals to the natural frequency of the cylinder
α	exponent index
δ_a, δ_s, δ_T	logarithmic decrement of aerodynamic, structural and total damping respectively
π	constant (= 3.14)
ρ	density of air
σ_y	standard deviation amplitude of motion of cylinder

2 INTRODUCTION

Mathematical models to predict the response of a large circular structure in natural wind flows have been developed by many previous researchers. The accuracy of these predictions relies on relatively simplistic theoretical models and frequently the applicability of the required input parameters to full scale situations at high Reynolds numbers and in turbulent flow. Some aerodyanmic parameters related to the wake excitation models have been measured in turbulent flows at high Reynolds numbers by Cheung and Melbourne (1983). However, this random wake excitation model has been shown by Kwok and Melbourne (1979) to be inadequate in the lock-in region and the simplification of assuming sinusoidal forcing does not reproduce satisfactorily the non-linear effect of lock-in, particularly at low values of structural damping. In the nineteen sixties, Scruton (1965) expressed the velocity dependent term of the aerodynamic force in a form of negative damping in conjuction with the structural damping. Although he has reported the non-linear negative aerodynamic damping has an effect on the limited amplitudes of oscillation, the experimental data published then were measured in smooth or subcritical flow, which precluded accurate predictions of full scale structural response at that time. Recently, Vickery and Basu (1983) incorporated this non-linear aerodynamic damping term in a more sophisticated mathematical model which can also incorporate the aeroelastic characteristics of spanwise correlation and the lock-in phenomenon. However, the lack of reliable data relevant to full scale configuration is still hampering the application of this semi-empirical prediction method. The dearth of measurements of aerodynamic damping for circular cylinders has prompted the present study with particular reference to its non-linear effects induced by the motion of the cylinder and by the turbulence in the flow at high Reynolds numbers.

3 EXPERIMENTAL ARRANGEMENTS

A series of experiments to measure the aerodynamic damping of a circular cylinder were carried out in the $1\frac{1}{2}$ m (height) by 1 m (width) by 2 m (length) insertable working section of the 450 kW closed circuit wind tunnel at Monash University. Grid turbulence was generated in the low speed sections of the wind tunnel so that high speed flows with various turbulence intensities and relatively constant longitudinal integral scale, $L_x \approx 90$ mm can be obtained in the test working section without stalling the wind tunnel fan. Reynolds numbers have been corrected for blockage effect according to Cheung and Melbourne (1980). Two cylinders of diameter 120 mm and 225 mm and of weight 2.1 kg and 3.0 kg respectively were used. The cylinders were made of poly-urethene around an aluminium tube, veneered with plywood and lacquered to provide rigidity. The final surface was polished with emery paper. The end plates were rectangular of three diameters wide and four diameters long and located 100 mm from the walls. A piece of acrylic fabric was used to seal each gap between the end plate and the model. The cylinder was suspended on different dynamic spring balance arrangements according to the natural frequency of the model required. The fluctuating force or oscillation of the cylinder was monitored by a four-armed bridge strain gauge system. The initial displacement of the cylinder was varied by hanging dead weights of various loads on the ends of the cylinder through a pulley system outside the wind tunnel working section as shown in Figure 1. As the cylinder is set to vibrate freely by unloading the dead weights instantly either with or without wind flow in the tunnel, the strain gauge signal is plotted on the Brush chart recorder or the Tetronix computer display

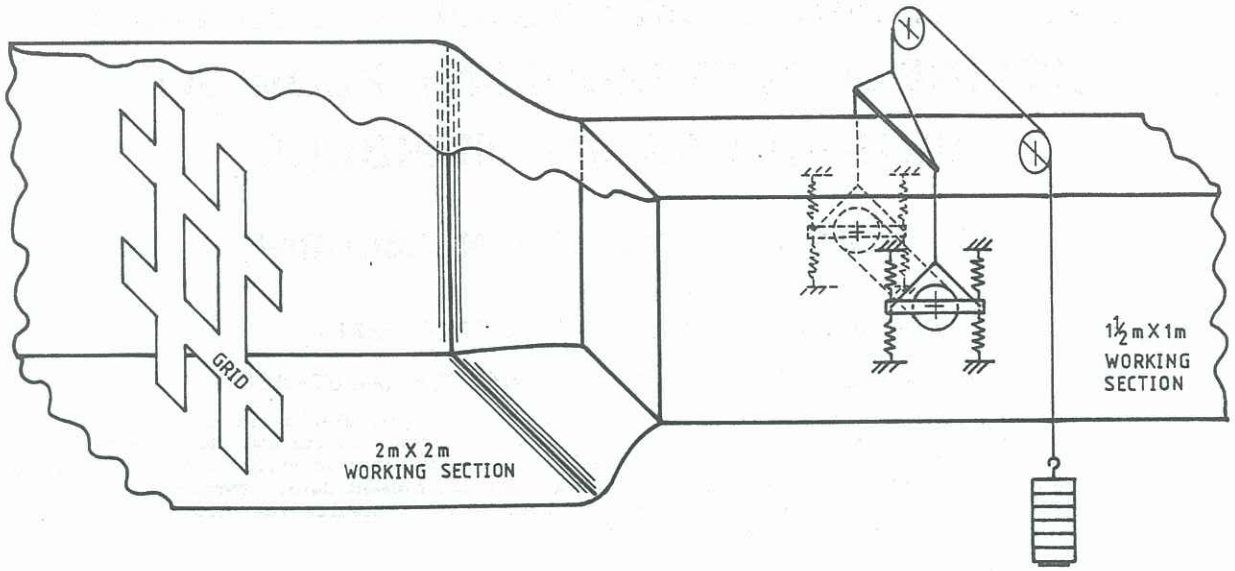

Figure 1 Schematic diagram showing the pulley system over the dynamic spring balance suspended with the cylinder in the high speed working section and the position of the grid in the low speed working section to generate turbulence without stalling the wind tunnel fan

unit. Typical signals recorded are shown in Figure 2. The logarithmic decrement of the total damping, $\delta_T = \delta_a + \delta_s$ can then be calculated for each of these cases. The aeodynamic damping is then obtained by subtracting the structural damping from the total damping.

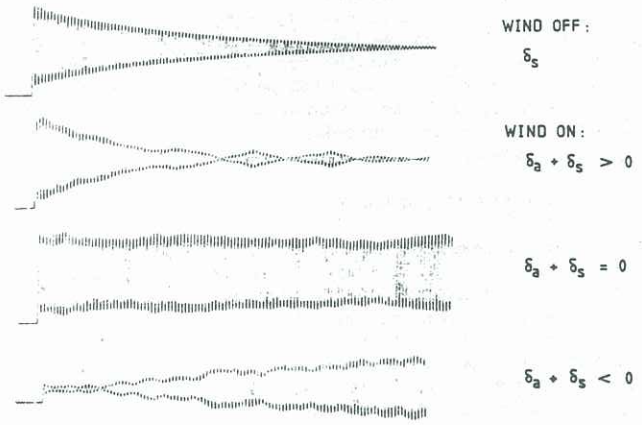

Figure 2 Typical damping curves obtained at different velocity ratios

4 RESULTS AND DISCUSSION

4.1 Effect of Amplitude of Motion

A typical plot of aerodynamic damping as logarithmic decrement versus velocity ratio for different amplitudes of the initial displacement of the cylinder in flows of turbulence intensity, I_u = 0.4% at Reynolds number of 0.31 x 10^5 is shown in Figure 3. For supercritical Reynolds numbers, the big cylinder was used and the critical velocity could only be obtained when the model was mounted on the dynamic balance with stiff spring suspension. Consequently, the variation of amplitude was too small for the evaluation of the effect of the amplitude dependence. Therefore, experiments for evaluating amplitude effects on aerodynamic damping were carried out with the small cylinder in the subcritical regime only.

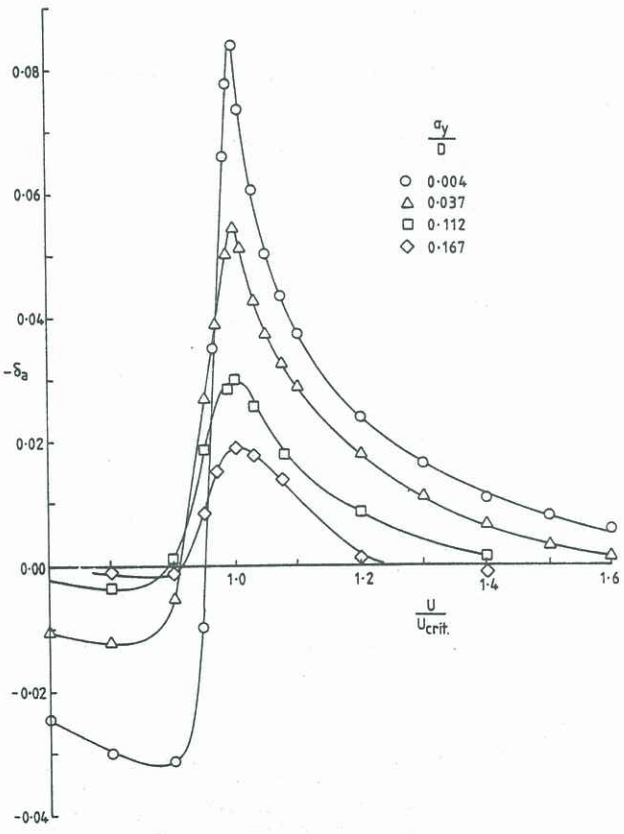

Figure 3 Aerodynamic damping coefficient versus velocity ratio for different amplitudes of the initial displacement of the cylinder in flows of turbulence intensity I_u = 0.4% at Reynolds number Re = 0.31 x 10^5

For subcritical flow and at critical velocity, Vickery (1978) has shown the effect of amplitude of motion on aerodynamic damping with limiting standard deviation amplitudes of 0.23 diameters and 0.3 diameters.

Scruton (1965) reported that the aerodynamic damping varies with the amplitude of motion hyperbolically and thus implied a larger limiting amplitude. In order to compare the present results with the existing ones, the present experimental data were fitted into the following equation of the same form as proposed by Vickery (1978) with a limiting standard deviation amplitude of motion of 0.3 of the diameter.

$$K_a = K_{a_o} \left[1 - \left(\frac{\sigma_y}{0.3D}\right)^{\alpha} \right]$$

K_{a_o} and α were then found from the best fit of each set of experimental data of K_a measured with a known value of σ_y in flows of different turbulence intensities and Reynolds numbers. α was found to be 0.32 for all cases with turbulence intensities varying from 0.4% to 9.1% in the Reynolds numbers range from 0.3×10^5 to 0.8×10^5. A comparison of the data fit with other workers is shown in Figure 4.

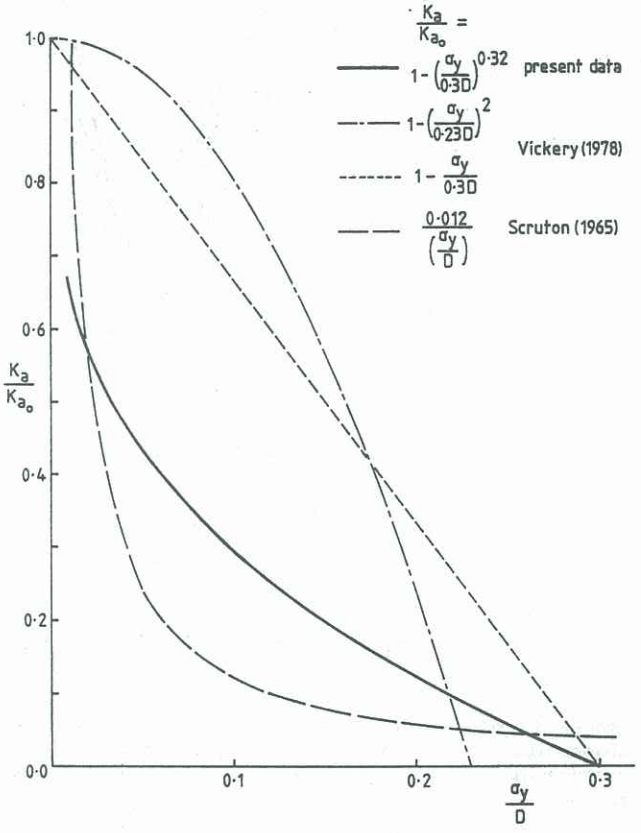

Figure 4 Comparison of data fit of $\left(\frac{K_a}{K_{a_o}}\right)$ versus $\left(\frac{\sigma_y}{D}\right)$, for $\frac{U}{U_{crit.}} = 1.0$

4.2 Effects of Velocity Ratio, Reynolds numbers and Turbulence intensities

As seen in Figure 3, the negative aerodynamic damping increases to a maximum at the critical velocity ratio and then decreases for smooth flow at subcritical Reynolds number. Positive aerodynamic damping is not found in turbulent flows or at high Reynolds numbers. All measured data of the aerodynamic damping K_a with motion σ_y were corrected for amplitude effect according to the equation described in the previous section to give the value K_{a_o} for a stationary circular cylinder. Figure 5 shows a plot of these corrected values for three levels of turbulence intensities at velocity ratios from 0.6 to 1.7 versus Reynolds numbers.

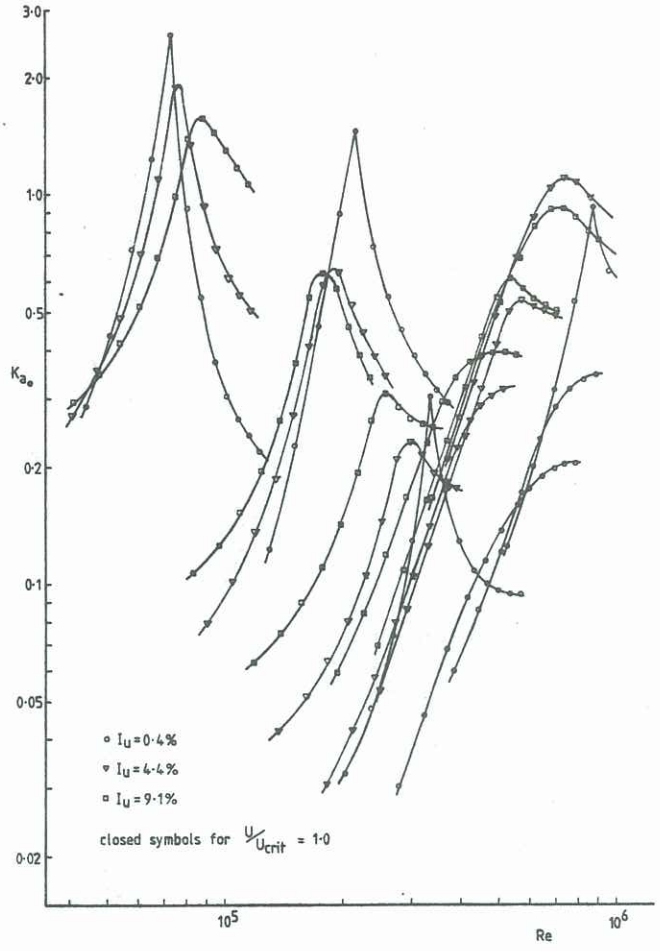

Figure 5 Negative aerodynamic damping versus Reynolds numbers for a stationary cylinder for three levels of turbulence intensities at velocity ratios from 0.6 to 1.7

By joining the points for critical velocity ratios only, Figure 6 is obtained, which shows a similar trend of Reynolds number effect as those found by Vickery (1978). It must be noted in Figure 5 that the Reynolds number changes as the velocity ratio is changed. Therefore, in order to examine the effect of velocity ratio at any particular Reynolds number, the points of the same velocity ratio must be joined up for various Reynolds number as shown in Figure 7. Then, a cross plot at any particular Reynolds number can be made. An example is shown in Figure 8 for three levels of turbulence intensity at a Reynolds number of 1×10^5. The negative aerodynamic dampings are thus corrected to zero amplitude and to the same Reynolds number even for different velocity ratios. As the turbulence intensity increases, the maximum negative aerodynamic damping is reduced and occurs at a higher velocity ratio. Also, the negative aerodynamic dampings increase with turbulence intensity at high velocity ratios, but decrease with turbulence intensities at velocity ratios below the critical.

5 CONCLUSION

The non-linear amplitude effect on the negative aerodynamic damping has been measured and shown to be described by the following equation

$$K_a = K_{a_o} \left[1 - \left(\frac{\sigma_y}{0.3D}\right)^{\alpha} \right]$$

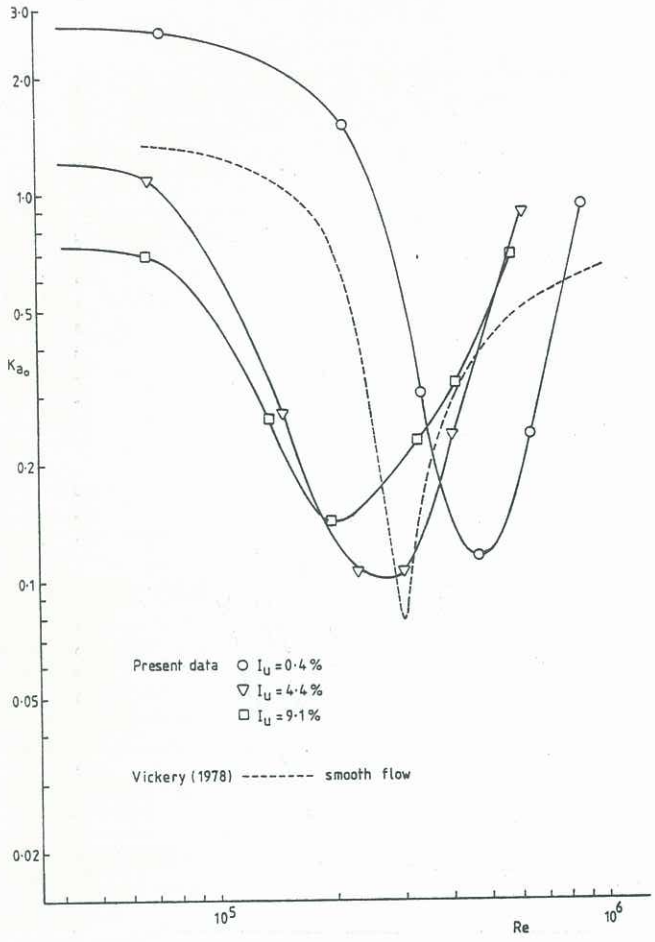

Figure 6 Aerodynamic damping coefficients K_{a_o} for a stationary circular cylinder at critical velocity ratio in flows of different turbulence intensities versus Reynolds number

where α = 0.32 for all turbulence intensities in the measured range of 0.4% to 9.1%. Positive aerodynamic damping is obtained below the critical velocity ratio in the subcritical regime, but cannot be found when the flow is turbulent or at high Reynolds numbers. Negative aerodynamic damping at the critical velocity ratio decreases with increasing turbulence intensity in the subcritical regime, but increases with turbulence in the supercritical range.

6 REFERENCES

CHEUNG, C.K. and MELBOURNE, W.H. (1980) Wind Tunnel Blockage Effects on a Circular Cylinder in Turbulent Flows. Proc. 7th Australasian Conf. on Hydraulics & Fluid Mechanics, Brisbane, pp. 127-130.

CHEUNG, J.C.K. and MELBOURNE, W.H. (1983) Turbulence Effects on Some Aerodynamic Parameters of a Circular Cylinder at Supercritical Reynolds numbers. Preprints of 6th Int. Conf. on Wind Engineering, Cold Coast, Australia, 2.

KWOK, K.C.S. and MELBOURNE, W.H. (1979) Cross-Wind Response of Structures due to Displacement Dependent Lock-In Excitation. Proc. 5th Int. Conf. on Wind Engineering, Fort Collins, Colorado, I, V-5-1.

SCRUTON, C. (1965) On the Wind-Excited Oscillations of Stacks, Towers and Masts. Proc. of Conf. on Wind Effects on Buildings and Structures, Teddington, Great Britain, pp. 798-836.

VICKERY, B.J. (1978) A Model for the Prediction of the Response of Chimney to Vortex Shedding. Proc. 3rd Int. Chimney Design Symp., Munich, Germany.

VICKERY, B.J. and BASU, R.I. (1983) Across-Wind Vibrations of Structures of Circular Cross-Section, Part 1 : Development of a Mathematical Model for Two-Dimensional Conditions. Jnl. of Wind Eng. and Industrial Aerodynamics, 12,49-73.

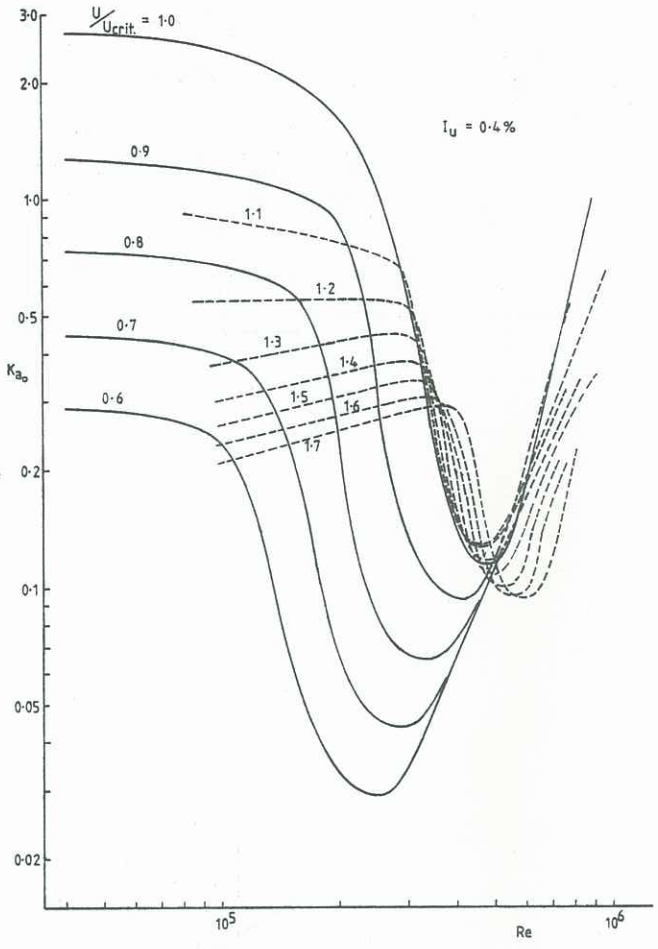

Figure 7 Negative aerodynamic damping versus Reynolds number for a stationary circular cylinder in a flow of turbulence intensity I_u = 0.4% for various velocity ratios

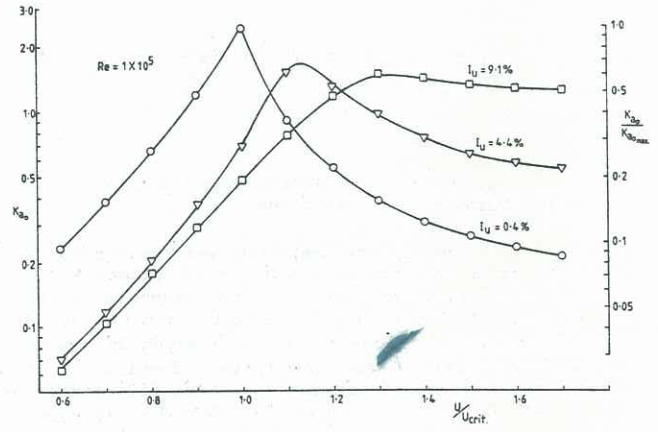

Figure 8 Negative aerodynamic damping versus velocity ratios for different turbulence intensities in a flow of Reynolds number Re = 1 x 10^5